Talanta 124 (2014) 79–88

Contents lists available at ScienceDirect

Talanta

journal homepage: www.elsevier.com/locate/talanta

Multielemental inductively coupled plasma optical emission spectrometry analysis of nickeliferous minerals

Elizabet Abad-Peña [a,1], María Teresa Larrea-Marín [b], Margarita Edelia Villanueva-Tagle [c], Mario Simeón Pomares-Alfonso [d,*,2]

[a] Department of Chemistry, Faculty of Natural Sciences, University of Oriente, Avenida Patricio Lumumba s/n, CP 90500, Santiago de Cuba, Cuba
[b] National Center of Metallurgical Researches (CENIM, CSIC), Avenida Gregorio del Amo, 8, 28040 Madrid, Spain
[c] Faculty of Chemistry, University of Havana, Calle Zapata s/n entre G y Mazón, Vedado, CP 10400, Havana, Cuba
[d] Institute of Materials Research and Engineering (IMRE), University of Havana, Calle Zapata s/n entre G y Mazón, Vedado, CP 10400, Havana, Cuba

ARTICLE INFO

Article history:
Received 18 October 2013
Received in revised form
29 January 2014
Accepted 31 January 2014
Available online 11 February 2014

Keywords:
Nickeliferous mineral
Matrix effect
ICP OES
Microwave-assisted digestion
Robust plasma
Matrix-matching calibration

ABSTRACT

An inductively coupled plasma optical emission spectrometry method for the quantitative simultaneous determination of Al, Ca, Co, Cu, Cr, Fe, K, Mg, Mn, Na, Ni, P and Zn in Cuban laterite and serpentine minerals has been developed. Additionally, V and Ti can be quantitatively determined in laterite mineral; Li, Sr, and Zr can be detected in both mineral types and Pb can be detected just in laterite mineral. The microwave-assisted total acid digestion of samples was achieved with $HCl+HNO_3+HF$ and HNO_3+HClO_4+HF acid mixtures for laterite and serpentine samples, respectively. In non-robust plasma operating conditions, the matrix effect characteristics of the laterite sample were dictated by the principal component Fe; while the character of the Mg principal component matrix effect was some how modified by the concomitants Fe and Ni in serpentine sample. The selection of robust conditions decreased the matrix effect. Additionally, the simulation of the matrix samples by introducing the principal component Fe or Mg, correspondingly, in calibration dissolutions was needed to overcome completely the matrix effect over the analysis accuracy. Precision of analysis was very near or lower than 10% for most elements, except Sr (15%) in L-1; and K (15%) and Li (15%) in SNi sample. Accuracy of analysis was around or lowers than 10% for most elements, except K (15%), Na (19%), P (19%) and V (19%) in L-1 sample; and Ca (14%) and P (20%) in SNi sample.

1. Introduction

The export of iron and cooper minerals from the west zone of Cuba began since 1902 by some foreigners companies such as the Bethlehem Steel Corporation. The deepest geological study on the presence of nickel in those ferruginous mineral deposits was carried out by researchers of the Padners Corporation (1939–1940). As result, the mineral body was characterized and the processing and extraction of nickel like matter has been prevailed since 1941 [1,2].

At present, the Cuban nickel deposits are recognized as one of the biggest in the world with, approximately, 37% of the nickel planet reserves. On the other hand, nickel industry represents one of the most important sectors of Cuban economy [3]. Seventy five thousand annual tons of nickel and cobalt mixture are currently produced from Cuban lateritic ores at three national hydrometallurgical plants. In connection with the prospecting and processing of this mineral, the determination of Ni, Co and Fe has been carried out at the geological chemical laboratories of the Republic of Cuba for more than forty years.

As known, inductively coupled plasma optical emission spectroscopy (ICP OES) is worldwide employed in geological studies [4,5]. Also, ICP OES has been routinely used for determination of Al, Co, Cr, Fe, Mg, Mn, Ni and Si in Cuban lateritic minerals since 1996, according to developed appropriate laboratory guidelines [6,7]. However, this mineral contains other elements, which should be determined as well because of several reasons. Particularly, the monitoring of Ca, Cu, K, Na, and Zn concentration is important in order to prevent their possible negative influence on the extraction metallurgical process of Ni plus Co concentrated product [8,9]. Additionally, the extension of the characterization of lateritic minerals to others elements, such as Cu, P and V, can contribute to a better evaluation of the mineral body [10].

According to the currently employed ICP OES methodology in Cuban laboratories [6,7], the sample test portion is digested by a

* Corresponding author. Tel.: +53 7 8781136.
E-mail addresses: elizabet@cnt.uo.edu.cu (E. Abad-Peña), m.larrea@cenim.csic.es (M.T. Larrea-Marín), villa@fq.uh.cu (M.E. Villanueva-Tagle), mpomares@imre.oc.uh.cu (M.S. Pomares-Alfonso).
[1] Present address: National Center of Metallurgical Researches (CENIM, CSIC), Avenida Gregorio del Amo, 8, 28040, Madrid, Spain.
[2] Postal address: Calle Zapata s/n entre G y Mazón, Vedado, CP 10400, Habana, Cuba.

http://dx.doi.org/10.1016/j.talanta.2014.01.066
0039-9140

fusion technique with lithium metaborate. Then, it is dissolved in hydrochloric or nitric acid dissolution. The addition of a significant amount of reagent to sample (sample:lithium metaborate=1:10) and the inherent laboriousness of the digestion procedure increases the risk of sample contamination and simultaneously reduces the net amount of sample to be analyzed. Consequently, an improvement of the limits of detections of determined analytes is not practically favoured.

In general, several alternative acid digestion procedures have been used instead of the fusion technique, prior to ICP OES elemental quantification of geological samples [11–16]. Among them, the microwave-assisted acid digestion has showed certain relevant characteristics such as, a shorter acid digestion time; better recovery of volatile elements and compounds, lower contamination levels, minimal volumes of reagents, more reproducible procedures and a better working environment. Generally, the proposed digestion methodologies involve two different acids combinations. In some reports [11–14], a mixture of nitric plus perchloric acids with a further addition of hydrofluoric acid, for the complete lixiviation of metals strongly linked to the crystalline lattice, has been employed. Also, a starting sample treatment with aqua regia ($HCl:HNO_3=3:1$), followed by the addition of hydrofluoric acid has been used [14,15]. The advantages or disadvantages of the both acid mixtures employed are not totally clear. In any case, the study and selection of an appropriate alternative acid digestion method of Cuban nickeliferous mineral for further ICP OES multielemental determination, including analytes at low concentration, is an important and necessary analytical task to be done.

On the other hand, an international recognized guideline standard method for the ICP OES analysis of nickeliferous minerals was not found in the reviewed literature. Moreover, ICP OES techniques have been relatively little reported [16–18] for the analysis of these minerals. Thus, the increment of the background intensity of the element spectral lines, caused by the high concentration of Fe, was compensated by matching Fe concentration in sample and calibration dissolutions [16]. In other work [17], ICP OES matrix effect was observed and further avoided by using the internal standard method. Finally, a simultaneous testing method for determination of few elements Ni, Co, Fe, Mg in laterite type Ni deposit was reported [18].

In this context, the aim of the current work was to carry out an analytical study for the determination of Al, Ca, Co, Cu, Cr, Fe, K, Li, Mg, Mn, Na, Ni, P, Pb, Sr, Ti, V, Zn and Zr in Cuban nickeliferous minerals by ICP OES. A special attention to the digestion of sample and matrix effect is given.

2. Materials and methods

2.1. Nickeliferous mineral samples

This work was focused on two types of Cuban nickeliferous minerals represented by the two reference materials (RMs), "Nickeliferous Laterite (L-1)" [19,20] and "Nickeliferous Serpentine (SNi)". Both RMs were manufactured at the Central Laboratory of Minerals José Isaac del Corral (LACEMI), as part of an international project with the participation of twenty eight laboratories from ten different countries. Eight diverse analytical techniques, Atomic Absorption Spectrometry, Inductively Coupled Plasma-Optical Emission Spectrometry, Colorimetry, Volumetry, Gravimetry, X-Ray Fluorescence, Potentiometry and DC Arc Atomic Emission Spectrography were employed in the certification process. The both types of selected minerals are the most important because they represent the 60% of the Cuban nickeliferous minerals with economical interest. On the other hand, the content of major elements of these two samples is extreme within the concentration interval of elements of the minerals that they represent. Thus, L-1 reference material is principally composed by 82% of goethite-FeO(OH), 6% of clay minerals, 5% of chromite-$FeCr_2O_4$ and 3% of serpentine-$Mg_3[Si_2O_5](OH)_4$; while SNi reference material is composed by 88% of serpentine-$Mg_3[Si_2O_5](OH)_4$, 7.5% of goethite-FeO(OH) and 2% of clay minerals. Concentrations of Ca, Cu, K, Na and P in SNi; and of Ca, K, Na, P and V in L-1 reference material, are given as approximated values, because of the high dispersion among concentrations reported by the participating laboratories. Nevertheless, they are still the best available reference concentrations that can be used for sake of statistical comparison with found concentrations.

2.2. Instrumentation

Microwave-assisted digestion of samples was carried out by using a Milestone ethos 1600 microwave lab station (Sorisole, Italy), which was operated at 2450 MHz and output energy of 900 W. Maximum temperature and pressure were of 300 °C and 100 bar, respectively. The microwave system is equipped with ten closed reaction vessels (100 mL capacity) made from polytetrafluoroethylene. The temperature inside the vessels was monitored by using a 300 Automatic Temperature Control Probe.

Measurements of the emission lines intensity were made in an axial view mode ICP OES SpectroArcos spectrometer (SPECTRO Analytical Instruments, Kleve, Germany) at operating parameters listed in Table 1.

2.3. Reagents and calibration dissolutions

65% Suprapur-grade Nitric acid (Merck, Darmstadt, Germany), 25% Suprapur-grade Hydrochloric acid (Panreac, Barcelona, Spain), 60% Suprapur-grade Perchloric acid (Merck, Darmstadt, Germany) and 48% Suprapur-grade Hydrofluoric acid (Panreac, Barcelona, Spain) were employed for sample digestion and/or dissolutions preparation; while the used deionised water of 18 $M\Omega\ cm^{-1}$ of resistivity was obtained with a Mili-*Q* system (Millipore, Bedford, MA, USA). Unielemental 10,000 mg L^{-1} CertiPURs standard dissolutions of Al, Ca, Fe, K, Mg, Mn Na, Ni, P, Ti, Zr; and 1000 mg L^{-1} of Co, Cu, Cr, Sr, Li, Zn, Pb, V (Merck, Darmstadt, Germany) were used for the preparation of calibration dissolutions and dissolutions used in the interference study.

For calibration purposes, two groups of multielemental dissolutions were prepared. The first group of five dissolutions contained six analytes, at the following concentration intervals: Al and Ni: 1–6 mg L^{-1}; Cr: 1.4–4 mg L^{-1}; Fe: 10–100 mg L^{-1}; Mg: 4–40 mg L^{-1}; Mn: 0.6–3 mg L^{-1}. The second group included three calibration dissolution subgroups. The first one, did not contain

Table 1
Operating conditions for Spectro ARCOS ICP optical emission spectrometer.

Parameter	Value
Nebulizer model	Modified Lichte
Spray chamber type	Glass, cyclonic
Injector ceramic tube internal diameter	2.5 mm
Read time	28 s
Radiofrequency incident power:	
• Highest MgII/Mg I	1400 W
• Lowest MgII/Mg I	900 W
Plasma argon flow rate	12 L min^{-1}
Nebulizer argon flow rate:	
• Highest MgII/Mg I	0.8 L min^{-1}
• Lowest MgII/Mg I	1.3 L min^{-1}
Auxiliary argon flow rate	1 L min^{-1}
Sample uptake rate	2 mL min^{-1}

matrix elements and the others two subgroups contained only Mg (1900 mg L^{-1}) and Fe (5000 mg L^{-1}), respectively; while concentration of nine analytes was the same in the three calibration dissolution subgroups. The concentration interval of analytes was: Ca: 1–20 mg L^{-1}; Co: 1–8 mg L^{-1}; Cu: 0.1–0.5 mg L^{-1}; K: 0.5–4 mg L^{-1}; Li and Sr: 1–10 mg L^{-1}; Na: 0.5–5 mg L^{-1}; P: 0.1–1.5 mg L^{-1}; Pb: 1–30 mg L^{-1}; Ti: 1–15 mg L^{-1}, V: 0.1–2.4 mg L^{-1}; Zn: 1–20 mg L^{-1} and Zr: 1–30 mg L^{-1}.

3. Results and discussions

3.1. Spectral interferences and line selection

A preliminary selection of the more sensitive lines of the nineteen elements Al, Ca, Co, Cu, Cr, Fe, K, Li, Mg, Mn, Na, Ni, P, Pb, Sr, Ti, V, Zn and Zr, initially considered in the present work, was made from the recommended database lines of the spectrometer software. The possible spectral interferences, produced by matrix elements Al, Cr, Fe, Mg, and Ni of both SNi and L-1 samples, were investigated over spectral lines of the remaining fourteen elements Ca, Co, Cu, K, Li, Mn, Na, P, Pb, Sr, Ti, V, Zn and Zr. With that purpose, the emission spectrum of each synthetic dissolution 1.5 and 1.9 (Table 2), that simulated the major elemental composition of L-1 and SNi samples, respectively, was visually compared to the spectrum of the corresponding matrix blank dissolution 2.5 and 2.9. Just the emission lines, free from spectral interferences (Table 3) were further considered.

3.2. Study and selection of plasma operating conditions

Generally, several parameters can be considered during the development of an ICP OES analytical methodology. However, in the present work the selection of the operating parameters is based on the study of the plasma robustness because of the strong and direct relationship between plasma robustness and the matrix effect; which is one of the most crucial limitations of the ICP OES analysis to be overcome [22]. Thus, selecting the robust plasma conditions should reduce the matrix effect and, consequently, the systematic error of analysis. In this context, it is useful to evaluate the behaviour of the plasma robustness with the variation of radiofrequency power and nebulizer argon flow rate; which are the principal parameters that exert a significant influence on the robustness.

As known [21], MgII 280.270 nm/MgI 285.213 nm (MgII/MgI) ratio is frequently used to evaluate the plasma robustness in ICP OES. In this work, MgII/MgI intensity ratio was measured during the nebulization of 10 mg L^{-1} magnesium dissolution for a total of sixty three radiofrequency power and nebulizer flow rate combinations. By keeping radiofrequency power constant at 0.9 kW, 1.0 kW, 1.1 kW, 1.2 kW, 1.3 kW, 1.4 kW and 1.5 kW; the nebulizer flow rate was varied at 0.5 L min^{-1}, 0.6 L min^{-1}, 0.7 L min^{-1}, 0.7 L min^{-1}, 0.9 L min^{-1}, 1.0 L min^{-1}, 1.1 L min^{-1}, 1.2 L min^{-1} and 1.3 L min^{-1}. The obtained tendencies of MgII/MgI as a function of F_N and P were similar to those previously reported [23–28]. As a result, the plasma robust conditions selected were $P=1.4$ kW and $F_N=0.8$ L min^{-1}; whereas the non-robust conditions were $P=0.9$ kW and $F_N=1.3$ L min^{-1}.

3.3. Matrix effect study

Dissolutions prepared for matrix effect study are shown in Table 2. The simulation of the elemental composition of sample dissolution was made by considering the total digestion of 0.250 g sample test portion in a final volume of 25 mL, and the further 1:100 dilution of the dissolved sample in 4% v/v HNO_3 before his introduction in the spectrometer. Thus, dissolutions 1.5 and 1.9 simulated the matrix of dissolved L-1 and SNi samples, respectively. The rest of type 1 dissolutions simulated the individual major element concentration contained in each of the dissolutions 1.5 and 1.9. All type 1 dissolutions contained, also, the analytes to be studied at concentration of 10 mg L^{-1} (group I: Cu, Na, K, Li and Sr) or 30 mg L^{-1} (group II: Ca, Co, Mn, P, Pb, Ti, Zn, Zr, and V). Type 2 dissolutions (from 2.1 to 2.9) were the matrix blanks of type 1 dissolutions. The dissolution 3 contained only the

Table 2
Dissolutions prepared for the study of spectral interferences, matrix effect and limits of detection.

Dissolution	Concentration (mg L^{-1})							HNO_3 (%, v/v)
	Matrix elements					Analytes		
	Al	Cr	Fe	Mg	Ni	Group I [a]	Group II [b]	
1.1	190	–	–	–	–	10	30	4
1.2	–	190	–	–	–	10	30	4
1.3	–	–	5000	–	–	10	30	4
1.4	–	–	–	–	110	10	30	4
1.5	190	190	5000	–	110	10	30	4
1.6	–	–	762	–	–	10	30	4
1.7	–	–	–	1900	–	10	30	4
1.8	–	–	–	–	190	10	30	4
1.9	–	–	762	1900	190	10	30	4
2.1	190	–	–	–	–	–	–	4
2.2	–	190	–	–	–	–	–	4
2.3	–	–	5000	–	–	–	–	4
2.4	–	–	–	–	110	–	–	4
2.5	190	190	5000	–	110	–	–	4
2.6	–	–	762	–	–	–	–	4
2.7	–	–	–	1900	–	–	–	4
2.8	–	–	–	–	190			4
2.9	–	–	762	1900	190	–	–	4
3	–	–	–	–	–	10	30	4
4	–	–	–	–	–	–	–	4

[a] Group I: Cu, Na, K, Li and Sr.
[b] Group II: Ca, Co, Mn, P, Pb, Ti, Zn, Zr, and V.

Table 3
Emission lines studied with the corresponding excitation energy for the atomic (I) and total excitation energy (excitation plus ionization energy) for the ionic (II) lines.

Element	Energy (eV)	Element	Energy (eV)	Element	Energy (eV)	Element	Energy (eV)
K(I) 766.491[a]	1.62	Zn(I) 213.586[d]	5.80	Zr(II) 272.262	11.35	Co(II) 228.616[a]	13.70
Li(I) 670.780	1.85	Mg(I) 202.647	6.12	V(II) 292.402	11.38	Co(II) 230.786[d]	13.75
Na(I) 589.592[a]	2.10	P(I) 178.287	6.95	Zr(II) 257.139	11.49	Ni(II) 231.604[a]	14.03
Na(I) 588.995	2.10	P(I) 177.495[a]	6.99	Mn(II) 260.569	12.19	Ni(II) 221.648	14.27
Sr(I) 460.733	2.69	Cu(I) 219.958	7.02	Mn(II) 259.373	12.21	V(II) 311.071[a]	14.49
Ca(I) 422.673 [b]	2.93	Al(I) 176.641	7.03	Mn(II) 257.611[a]	12.24	Ca(II) 183.801[b]	14.55
Al(I) 396.152	3.14	P(I) 214.914[c]	7.18	Cr(II) 284.325	12.63	Pb(II) 172.680	14.60
Al(I) 394.401	3.14	P(I) 213.618	7.21	Cr(II) 284.984	12.66	Pb(II) 168.215	14.78
Ti(I) 334.187	3.71	Zn(I) 334.502	7.78	Cr(II) 283.563	12.69	Pb(II) 220.353	14.79
Na(I) 330.298	3.75	Sr(II) 421.552	8.63	Fe(II) 261.187	12.69	Zn(II) 206.200[a]	15.41
Cu(I) 327.396[a]	3.79	P(I) 169.403	8.73	Mn(II) 294.921	12.81	Zn(II) 202.613[b]	15.51
Cu(I) 324.754[b]	3.82	P(I) 168.599	8.76	Cr(II) 267.716[a]	12.95	Fe(II) 244.451	15.55
Li(I) 323.261	3.83	P(I) 138.147	8.98	Fe(II) 238.204	13.10	Cu(II) 224.700[d]	15.96
Mg(I) 285.213	4.35	Zr(II) 343.823	10.33	Fe(II) 239.562	13.12	Fe(II) 259.941[a]	16.09
Pb(I) 283.305	4.36	Zr(II) 339.198	10.45	Ca(II) 315.887	13.16	Cu(II) 219.226[d]	16.21
Pb(I) 405.778	4.36	Ti(II) 336.121[a]	10.54	Ca(II) 317.933[a]	13.16	Mg(II)279.079[a]	16.51
Li(I) 274.118	4.52	Ti(II) 334.941	10.58	Al(II) 167.078[a]	13.41	Pb(II) 167.153	16.58
Li(I) 460.289	4.54	Ti(II) 323.452	10.71	Co(II) 238.892[d]	13.48		
Pb(I) 261.418	5.71	V(II) 292.464	11.34	Co(II) 237.862[b]	13.51		

[a] Analytical line selected for the final analysis. Spectral lines that were interfered by one of the following major components [b] Al, [c] Fe, [d] Mg, and/or [e] Ni were not used to study the matrix effect caused by that specific interfering major component.

analytes to be studied at the same concentration than type 1 dissolution. Finally, the dissolution 4 was the blank of dissolution 3. All dissolutions were prepared at 4% (v/v) HNO_3.

Matrix effect on free from spectral interferences analytical lines of analytes included in Table 3 was calculated, in percentage, according to Eq. (1)

$$ME = \left[\left(\frac{I_1 - I_2}{I_3 - I_4}\right) - 1\right] \times 100 \quad (1)$$

where, I_1, I_2, I_3 and I_4 were measured in the corresponding dissolution. Four replicates of each dissolution were measured at two different times during a working day; hence, the calculated ME was the mean of eight replicates.

In a first approach, the average of the absolute matrix effect over all studied analytical lines in Table 3 due to sample complex matrices and their single components Al, Cr, Fe, Mg and Ni, was evaluated in robust and non-robust plasma operating conditions by using synthetic dissolutions described in Table 2. In non-robust conditions, average matrix effect were significantly high, for both sample complex matrices (Fe+Mg+Ni and Al+Cr+Fe Ni mixtures); and also for individual Mg (1900 mg L^{-1}), Fe (762 mg L^{-1}) and Fe (5000 mg L^{-1}) matrices; while it was not significantly (~ 10%) in the presence of single 190 mg L^{-1} Al, 190 mg L^{-1} Cr and 110 mg L^{-1} Ni matrices.

In robust conditions the average matrix effect was reduced. Obviously, from the practical point of view, if a better accuracy is desirable, then the use of non-robust condition has to be discarded. Nevertheless, a closer look to the effect in non-robust and the comparative study with the effect in robust conditions can facilitate the comprehension of the ICP OES matrix effect mechanisms; which are not totally understood from the theoretical point of view. In this context, the present study is useful and also novelty because the experimental evidences reported for matrix effect in ICP OES analysis of laterite and serpentine are very scarce in comparison with the effects reported for samples with others principal components such as, Ca, Mg and easily ionized elements [24,29–31]. Consequently, a meticulous study of the dependence of the matrix effect with the total excitation energy of analytical lines (ME vs. TEE relationship) was carried out in non-robust (Fig. 1) and robust conditions (Fig. 2) for the individual Fe (762 mg L^{-1} and 5000 mg L^{-1}), Mg (1900 mg L^{-1}) and for the both matrix elements mixtures.

In non-robust conditions (radiofrequency power=0.9 kW, nebulizer argon flow=1.3 L min^{-1}), intensity of most lines increased in the presence of laterite (Fig. 1a) and serpentine (Fig. 1b) simulated matrices, but the behaviour of the effect with the total energy excitation of lines depended of sample type. In the case of laterite, the effect was significant for most lines with energies in the intervals of approximately 1.62–4.0 eV and 10.0–16.0 eV (Fig. 1a); while no effect was observed for lines with energies around 7–9 eV. The high concentration of Fe decided, with no doubts, the conduct of matrix effect in laterite. Note that in the sole presence of Fe at two differente concentrations (Fig. 1c) a similar behaviour was observed. In both samples (Fig. 1a and c) the correlation between effect and energy lines was not significant. For Fe matrix (Fig. 1a), those results have not been reported in the reviewed literature [25,29,30,34]. In contrast with the results obtained for laterite matrix, the effect of serpentine simulated matrix (Fig. 1b) and individual Mg (Fig. 1d) was also significant for some lines with energy around 8 eV. However, the most interesting difference between serpentine and laterite matrix effect is the ME vs. TEE statistical significant dependence observed in serpentinite for energy lines lower than, approximately, 8 eV. In this case (Fig. 1b) a correlation coefficient (R^2) of 0.63 was statistically significant for a 95% of probability with 12 degree of freedoms. Another difference respect to the ME vs. TEE behaviour of laterite and the principal role played by Fe in it is the surprising difference between the ME vs. TEE behaviour of serpentine and the principal component Mg. It should be noted that no correlation between ME of Mg and TEE of lines with energies lower than 8 eV was observed (Fig. 1d). Therefore, the appearance of some interaction effect among matrix elements in Fe+Mg+Ni serpentine sample is warranted. This interaction should be, principally, between Fe and Mg, according to the relatively high concentrations of those elements, 762 mg L^{-1} and 1900 mg L^{-1} respectively, in comparison to the low 190 mg L^{-1} concentration of Ni. Obviously, the Fe/(Al+Cr+Fe+Ni)=0.91 concentration ratio in laterite, which is higher than the corresponding to serpentine Mg/(Fe+Mg+Ni)=0.69 ratio, can be the responsible for the differences of the observed behaviour. A more detailed theoretical explanation is out the scope of the present work and requires additional experiments.

In robust conditions (radiofrequency power=1.4 kW, nebulizer flow argon=0.8 L min^{-1}), beside the sensible reduction of the effect already mentioned before a drastic change in the effect type (enhancement or reduction of line intensity) and in the ME vs. TEE relationship was observed (Fig. 2). First, higher effects were observed for lines with energies in the extremes (around 2 eV

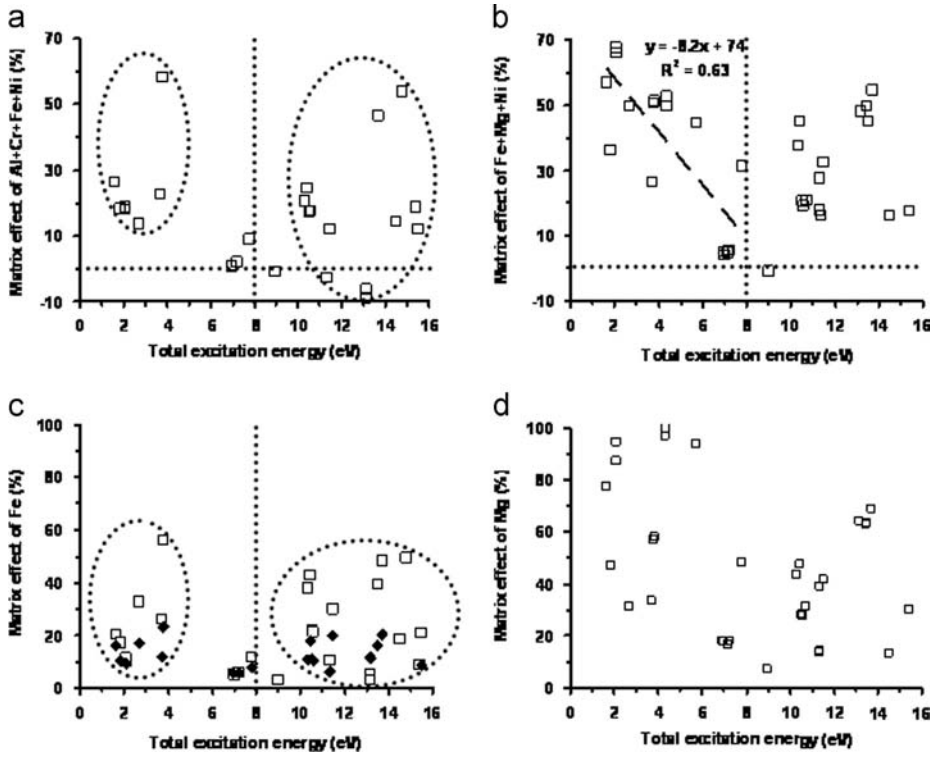

Fig. 1. Variation of the matrix effect (ME) with the total excitation energy (TEE) of line in non-robust conditions (P=0.9 kW and F_N=1.3 L min^{-1}) for: (a) combined Al (190 mg L^{-1})+Fe (5000 mg L^{-1})+Cr (190 mg L^{-1})+Ni (110 mg L^{-1}) matrix; (b) combined Fe (762 mg L^{-1})+Mg (1900 mg L^{-1})+Ni (190 mg L^{-1}) matrix; (c) individual Fe (□-5000 mg L^{-1}, ♦-762 mg L^{-1}) matrices; individual Mg (1900 mg L^{-1}) matrix.

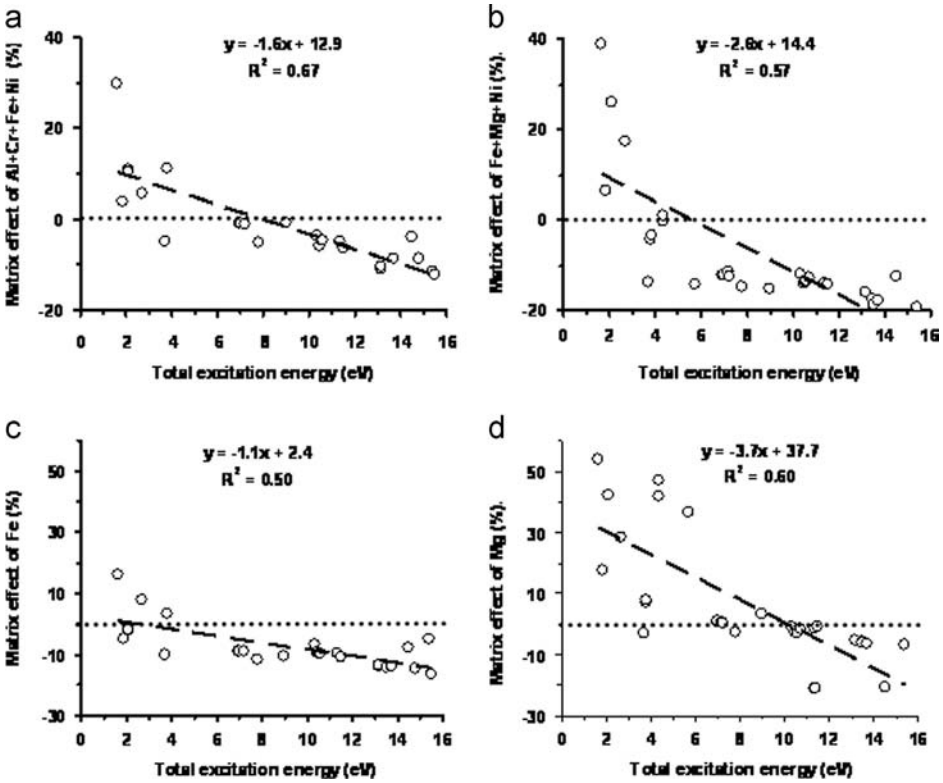

Fig. 2. Variation of the matrix effect (ME) with the total excitation energy (TEE) of line in robust conditions (P=1.4 kW and F_N=0.8 L min^{-1}) for: (a) combined Al (190 mg L^{-1})+Fe (5000 mg L^{-1})+Cr (190 mg L^{-1})+Ni (110 mg L^{-1}) matrix; (b) combined Fe (762 mg L^{-1})+Mg (1900 mg L^{-1})+Ni (190 mg L^{-1}) matrix; (c) individual Fe (5000 mg L^{-1}) matrix; (d) individual Mg (1900 mg L^{-1}) matrix.

and 16 eV) of the energy interval, but intensity of lines with higher energies decreased contrary to the increment occurred for the same lines in non-robust conditions. Second, matrix effect was directly proportional to the line energy for the combined Al+Cr+Fe+Ni (Fig. 2a) and Fe+Mg+Ni (Fig. 2b); and for the individual Fe (Fig. 2c) and Mg (Fig. 2d) investigated matrices, with

Table 4
Microwave-assisted heating programs.

Sample	Program		Parameter	Steps								Total Time (min)	
				1	2	3	4	5	6	7	8		
SNi	1		Power (W)	250	0	400	0	650	250	0	–		30
			Time (min)	5	5	5	5	3	2	5	–		
	2		Power (W)	250	0	400	0	600	0	250	0		35
			Time (min)	5	5	5	5	3	5	2	5		
L-1	3		Power (W)	250	0	600	0	600	0	–	–		27
			Time (min)	10	2	3	4	3	5	–	–		
	4		Power (W)	250	0	600	0	600	0	600	0		36
			Time (min)	10	2	4	4	4	4	3	5		
	5	5.1	Power (W)	250	0	650	0	–	–	–	–	21	46
			Time (min)	10	2	4	5	–	–	–	–		
		5.2	Power (W)	350	0	350	0	–	–	–	–	25	
			Time (min)	10	5	5	5	–	–	–	–		
	6	6.1	Power (W)	250	0	450	0	650	0	–	–	37	49
			Time (min)	10	2	10	5	5	5	–	–		
		6.2	Power (W)	250	0	–	–	–	–	–	–	12	
			Time (min)	10	2	–	–	–	–	–	–		

Table 5
Digestion procedures investigated.

Sample	Digestion procedure	Mixture	Acid volume (mL)				Total volume (mL)	Microwave heating program
			HNO_3	$HClO_4$	HF	Aqua Regia		
SNi	D-1	1	5[a]	2	1	–	8	1 and 2
	D-2	2	5[b]	2	1	–	8	1 and 2
	D-3	3	2[c]	2	1	–	5	1
L-1	D-4	4	–	–	3	3	6	3
	D-5	5	–	–	3	3.5	6.5	4
	D-6	6	–	–	3	4	7	5
	D-7	7	–	–	3	4.5	7.5	6

[a] 5 mL of HNO_3:H_2O (1:1).
[b] 5 mL of HNO_3:H_2O (2:1).
[c] 2 mL of concentrated 65%HNO_3.

statistically significant correlation coefficients of 0.67, 0.57, 0.50 and 0.60, respectively. Precisely, the found correlation between matrix effect and total excitation energy of lines, allow assuring that the observed effect is predominantly related to the plasma excitation mechanisms of lines and not to others possible matrix effects generated during the introduction and transportation processes of sample into the plasma. The observed correlations in laterite and serpentine at robust conditions were similar to that reported for single Al, Ca and Mg matrices [32]; and for a complex, Pb+Zr+Ti+Sr matrix [33]. Again, this ME vs. TEE behaviour in robust condition seems to be no dependent of major element type.

Once the preliminary selection of the robust operating plasma parameters was done, a sample digestion procedure will be implemented.

3.4. Microwave-assisted acid digestion of samples

Six microwave-assisted heating programs, two for SNi; and four for L-1 were designed (Table 4). In programs 5 and 6, the samples were consecutively treated twice by using 5.1 and 5.2; and 6.1 and 6.2 subprograms, respectively.

According to the mineralogical composition of samples and the reviewed literature [11–15], the HNO_3+$HClO_4$+HF and aqua regia+HF acid combinations were studied for SNi and L-1 digestion, respectively. For SNi sample, HNO_3 concentration was varied from 32.5% (mixture 1) up to 65% (mixture 3); while $HClO_4$ and HF acid volumes were constant (Table 5). For L-1 sample, aqua regia varied from 3 mL to 4.5 mL; while HF was kept constant. The used volumes of HF for each sample were selected in a previous experiment by evaluating, visually, the presence or absence of a precipitate; while, the others reagents were kept constant. Thus, a total of seven digestion options, three (D-1–D-3) for SNi; and four, (D-4–D-7) for L-1 were studied (Table 5). In D-1 and D-2 SNi procedures two consecutive heating programs were applied. Heating program 1 was run after addition of nitric acid to sample. After sample reached room temperature, similar amounts of HF (1 mL) and $HClO_4$ (2 mL) were successively added and then, the heating program 2 was run. In the D-3 procedure, HNO_3, $HClO_4$ and HF were successively added to sample. Then, the program 1 was run. For L-1 sample, the aqua regia+HF acid mixture was added to 250 mg of sample and, immediately, the corresponding program, was run. The total elimination of the HF acid residue from the sample dissolution was guaranteed by adding and heating, repeatedly, 0.5 mL of $HClO_4$ until white vapours disappeared. Finally, dissolved samples were raised up to 25 mL with 4% (v/v) HNO_3 dissolution. Five replicates of sample portions were digested in parallel and each replicate was measured six times at routine plasma conditions radiofrequency power=1.4 kW and nebulizer flow gas=1.0 L min^{-1}. Others parameters were listed in Table 1. The procedures were evaluated by comparing the found concentration in sample dissolution with the concentration of matrix elements reported in the certificate.

As can be seen in Table 6, the total content of Al, Cr, Fe, Mg and Ni was totally transferred into dissolution, within the experimental error, when samples were digested by using the D-3 procedure. Thus, the increment of HNO_3 concentration favoured, particularly,

the total dissolution of Ni. Concerning L-1 sample, the content of Al, Fe, Mg and Ni was quantitatively recovered just by the procedure D-7; while Cr found concentration was lower than reference one.

According to the obtained results, D-3 and D-7 procedures were selected, in a first approach, for SNi and L-1 samples digestion, respectively.

3.5. Influence of plasma robustness on precision of analysis

The relationship between plasma robustness and matrix effect, and indirectly with the accuracy of analysis is well documented in the literature; however, experimental evidences of the influence of the robust conditions on the precision of the analysis are scarce [24,29,34]; and no references of such reports were found for nickeliferous minerals ICP OES analysis [5,16–18]. In this work, the influence of plasma robustness on precision of determination of Al, Cr, Fe, Mg, Mn and Ni was evaluated in non-robust and robust operating plasma conditions for SNi and L-1 samples. Precision was estimated as the relative standard deviation (RSD) of concentration for six replicates. In sample L-1, precision was more sensitive to plasma robustness than that in sample SNi. Reduction of RSD in robust conditions was notable for mostly elements in L-1 sample; while precision was improved just for Cr and Mn in SNi sample. For all elements in both samples precision was lower than 5% in the robust conditions. The improvement of precision also justifies the selection of robust conditions.

3.6. No matrix-matching and matrix-matching calibration curves.

The use of the same no matrix-matching calibration curves (without matrix) for the analysis of Ca, Co, Cu, K, Li, Na, P, Pb, Sr, Ti, V, Zn and Zr in both SNi and L-1 samples would be very attractive. However, the presence of a remaining matrix effect in robust conditions, previously discussed in Section 3.3, could affect the accuracy. Therefore, analysis was made by using the both types of calibration curves for comparison purposes (Table 7).

In a first approach, let to evaluate the determination of Ca, Co, Cu, K, Li, Na, P, Pb, Sr, Ti, V, Zn and Zr in both SNi and L-1 samples by using no matrix-matching calibration curves. In SNi sample analysis, found concentration of Ca, Cu, K, P, Na and Zn was similar to reference concentrations; while concentration of Co was lower than that and Pb was not detected (see columns 5 and 7 in Table 7). On the other hand, reference concentration of Li, Sr, Ti, V

Table 6
Evaluation of digestion procedures for SNi and L-1 sample analysis.

Sample	Element	Reference concentration	Found concentration ± confidence interval ($n=5$, $\alpha=0.05$) in %, m/m						
			D-1	D-2	D-3	D-4	D-5	D-6	D-7
SNi	Al	0.49 ± 0.03	0.48 ± 0.03	0.54 ± 0.02	0.51 ± 0.02	–	–	–	–
	Cr	0.40 ± 0.02	0.38 ± 0.03	0.31 ± 0.01	0.40 ± 0.01	–	–	–	–
	Fe	7.6 ± 0.1	7.5 ± 0.3	7.54 ± 0.03	7.6 ± 0.1	–	–	–	–
	Mg	19.2 ± 0.3	19 ± 1	18.8 ± 0.3	20.4 ± 1.1	–	–	–	–
	Ni	1.92 ± 0.03	1.8 ± 0.1	1.76 ± 0.02	1.9 ± 0.1	–	–	–	–
L-1	Al	1.9 ± 0.1	–	–	–	1.82 ± 0.04	1.8 ± 0.1	1.7 ± 0.1	1.79 ± 0.04
	Cr	1.97(1.89–1.99)[b]	–	–	–	1.67 ± 0.04	1.64 ± 0.03	1.49 ± 0.02	1.68 ± 0.03
	Fe	52.9 ± 0.2	–	–	–	51.6 ± 0.6	52 ± 1	52.0 ± 0.4	52.1 ± 0.7
	Mg	0.41 ± 0.03	–	–	–	0.40 ± 0.02	0.39 ± 0.02	0.39 ± 0.01	0.41 ± 0.01
	Ni	1.15 ± 0.02	–	–	–	1.05 ± 0.01	1.05 ± 0.01	1.06 ± 0.01	1.1 ± 0.1[a]

[a] Confidence interval of Ni in L-1 digested by D-7 procedure was calculated for a confidence level $\alpha=0.01$.
[b] Median (Median interval).

Table 7
Average concentration ± confidence interval ($n=5$, $\alpha=0.05$) in mg kg^{-1} determined in robust conditions by using matrix-matching and no matrix-matching calibration curves.

Element	L-1 sample			SNi sample		
	Reference concentration [a]	Found concent. ± confidence interval [b]		Reference concentration [a]	Found concent ± confidence interval [b]	
		Fe-matching	No matrix-matching		Mg-matching	No matrix-matching
Ca	643 ± 622	567 ± 83	315 ± 3	1700 (1275–3329)	1945 ± 33	1450 ± 103
Co	740 (710–750)	698 ± 15	581 ± 5	150 ± 8	147 ± 5	104 ± 7
Cu	42.6 ± 3.6	39.4 ± 0.4	40 ± 1	21[c]	21 ± 3	18 ± 3
K	332 ± 184	283 ± 5	287 ± 3	62 ± 947	52 ± 8	156 ± 14
Na	445 ± 269	531 ± 99	606 ± 1	117 ± 126	117 ± 2	152 ± 24
P	118 ± 100	97 ± 6	85 ± 1	90 (11–1803)	72 ± 5	65 ± 6
Ti	707 ± 61	763 ± 15	727 ± 8	No reported	329 ± 8	408 ± 12
V	183 ± 43	148 ± 7	122 ± 1	No reported	41 ± 2	37 ± 5
Zn	317 ± 48	299 ± 38	268 ± 3	82 ± 15	88 ± 10	89 ± 15
Li	4[d]	5.7 ± 0.2	5.5 ± 0.2	No reported	1.0 ± 0.2	1.1 ± 0.2
Pb	37 ± 3	8.4 ± 0.3	7.7 ± 0.2	No reported	< 0.7	< 0.7
Sr	16[d]	5 ± 1	5 ± 1	No reported	2.5 ± 0.1	2.5 ± 0.1
Zr	75[d]	20.4 ± 0.3	18.6 ± 0.3	No reported	0.6 ± 0.1	0.8 ± 0.1

[a] For Ca and P in SNi; and for Co in L-1, reference concentration is expressed as median (median interval).
[b] For Co and V in SNi; and Ca in L-1, confidence interval of found concentration was calculated with $\alpha=0.01$.
[c] Only median concentration is provided for Cu.
[d] Confidence interval of the average concentration was not provided

and Zr are not given in the certificate. For these elements, except Ti, found concentrations determined by using Mg-matching and no matrix-matching calibration curves were equals within the experimental error; which confirmed the absence of systematic error. Concentration of Ti, determined by using the Mg-matching calibration curves can be considered as the best result for this element in SNi sample. In L-1 sample analysis, found concentration was lower than reference one for Co, Pb, Sr, Zr and V; while it was higher for Li. For the remaining seven elements Ca, Cu, K, Na, P, Ti and Zn, the differences between found and reference concentration was not significantly (see columns 4 and 2 in Table 7).

Further, a second approach by using matrix-matching calibration curves was investigated. Thus, 1900 mg L^{-1} of Mg and 5000 mg L^{-1} of Fe were added, separately, to the both calibration dissolutions set for SNi and L-1 samples, respectively. With the use of Mg-matching calibration curve for SNi sample analysis, found concentration of Co became similar to the reference one; while the good results for Ca, Cu, K, P, Na and Zn, previously obtained by using no matrix-matching curves, did not change (columns 6 and 5 in Table 7). In sample L-1, the use of the Fe-matching calibration curves reduced the systematic error of analysis for Co and V; while found concentrations of Li, Pb, Sr and Zr were still different from the reference ones. For the rest of elements (Ca, Cu, K, Na, P, Ti and Zn), found concentration determined with Fe-matching curves, kept similar to reference ones as it was obtained with the no matrix-matching calibration curve (columns 3 and 2 in Table 7).

In conclusion, the Fe-matching and Mg-matching curves should be used additionally to the selected robust conditions for a better reduction of the systematic error caused for the matrix effect.

3.7. Evaluation of the method performance parameters

In order to provide the first analytical information of the characteristics of the developed methodology, the most important performance parameters, accuracy, precision and limit of detection were evaluated. A full validation process will be carry out in the specific conditions of the geological service laboratory; in which the methodology will be implemented with routine analysis purposes. According to the previous results, robust operating parameters of the plasma were fixed and the Mg-matching and Fe-matching calibration curves for SNi and L-1 reference materials, respectively, were used.

As can be seen in Table 8, no significant differences were observed between found and references concentration for mostly elements in both samples. Statistical evaluation was made by applaying the *t*-Student test for a confidence level of $\alpha=0.05$ or $\alpha=0.01$and six determinations. For some elements, statistical comparison was made by the overlapping of the provided median confidence intervals. In sample L-1, some exceptions were observed: found concentration of Cr was significantly low because of the insufficient extraction of this element; which was observed previously in (see Table 6 in Section 3.4); found concentration of Pb was also lower than reference one. Some association between Cr and Pb in L-1 sample could explain this fact. Nevertheless, additional work has to be done in order to improve the Cr and Pb analysis. Li, Sr and Zr in L-1 were not evaluated because of the confidence interval of reference concentration was not provided. In sample SNi good agreement between found and reference concentration was established, except for Li, Sr, Pb, Ti and V; for which reference concentrations were not given.

Finally, the principal performance parameters of the developed methodology were calculated and given in Table 9. The accuracy error was estimated as the percentage difference between the mean concentration found by using the developed methodology and the reference concentration. In L-1 sample, accuracy error was around or lower than 10% for most of elements (Ca, Co, Cr, Cu, Ti, Zn, Al, Cr, Fe, Mg, Mn and Ni), except K (15%), Na (19%), P (19%) and V (19%). It is important to note, that, in spite of the confidence interval of Cr found concentration in sample L-1 did not overlapped the confidence interval of the median reference concentration of Cr in reference material (see Table 8), the accuracy error was relatively low (9%). Because of that reason, it is reasonable and practical to consider the determination of Cr in L-1 as quantitative

Table 8
Statistical assessment of systematic errors. Reference and found concentration are expressed in %, m/m (Al, Cr, Fe, Mg, Mn and Ni) or in mg kg^{-1} (Ca, Co, Cu, K, Li, Na, P, Pb, Sr, Ti, V, Zn and Zr).

Element	L-1 reference material				SNi reference material			
	Reference concentration[a]	Found concentration[b]	$t_{experimental}$	t_{table}	Reference concentration[a]	Found concentration[b]	$t_{experimental}$	t_{table}
Ca	643 ± 622	567 ± 83	0.13	2.16	1700 (1275–3329)	1945 ± 33	[c]	[c]
Co	740 (710–750)	698 ± 15	[c]	[c]	150 ± 8	147 ± 5	0.4	2.08
Cu	42.6 ± 3.6	39.4 ± 0.4	1.1	2.10	21	21 ± 3	0.3	2.57
K	332 ± 184	283 ± 5	2.35	2.92	62 ± 947	52 ± 8	0.03	2.26
Li	4[d]	5.7 ± 0.2	–	–	No reported	1.0 ± 0.2	–	–
Na	445 ± 269	531 ± 99	0.36	2.18	117 ± 126	117 ± 2	0.01	2.26
Sr	16[d]	5 ± 1	–	–	No reported	2.5 ± 0.1	–	–
P	118 ± 100	97 ± 6	0.9	2.13	90 (11–1803)	72 ± 5	[c]	[c]
Pb	37 ± 3	8.4 ± 0.3	3.62	2.18	No reported	< 0.7	–	–
Ti	707 ± 61	763 ± 15	1.0	2.06	No reported	329 ± 8	–	–
V	183 ± 43	148 ± 7	1.9	2.18	No reported	41 ± 2	–	–
Zn	317 ± 48	299 ± 38	0.6	2.08	82 ± 15	88 ± 10	2.0	2.18
Zr	75[d]	20.4 ± 0.3	–	–	No reported	0.6 ± 0.1	–	–
Al	1.9 ± 0.1	1.8 ± 0.1	1.6	2.04	0.49 ± 0.03	0.43 ± 0.03	2.07	2.13
Cr	1.97 (1.89–1.99)	1.79 ± 0.03	[c]	[c]	0.40 ± 0.03	0.35 ± 0.03	2.58	2.92
Fe	52.9 ± 0.2	53 ± 1	1.5	2.04	7.6 ± 0.1	7.5 ± 0.2	1.6	2.06
Mg	0.41 ± 0.02	0.42 ± 0.02	0.0	2.04	19.2 ± 0.3	18.9 ± 0.2	1.5	2.86
Mn	0.62 ± 0.01	0.63 ± 0.02	1.1	2.02	0.11 ± 0.01	0.10 ± 0.01	0.2	2.09
Ni	1.15 ± 0.02	1.2 ± 0.1	0.9	2.04	1.92 ± 0.03	1.92 ± 0.01	0.13	2.02

[a] Reference concentration is expressed as average concentration ± confidence interval, with the exception of Co and Cr in L-1; and Ca and P in SNi, for which it is expressed as median concentration (median interval).
[b] Confidence interval of found concentration was calculated with $n=6$ and $\alpha=0.05$, except K in L-1; and Al and Cr in SNi; for which was calculated with $n=6$ and $\alpha=0.01$.
[c] Statistical comparison was made by the overlapping (or not overlapping) of the median confidence intervals.
[d] Confidence interval for Li, Sr and Zr in L-1 sample is not given.

Table 9
Performance parameters of the developed analytical procedure.

Element	L-1 reference material			SNi reference material		
	Accuracy (%)	Precision (%)	LOD[a] (mg kg^{-1})	Accuracy (%)	Precision (%)	LOD[a] (mg kg^{-1})
Ca	12	11	8	14	1.6	0.7
Co	6	2.2	0.08	2.0	3.2	0.2
Cu	8	0.5	0.1	1.9	14	0.2
K	15	1.4	0.3	16	15	0.9
Na	19	5.9	0.2	0.4	1.6	0.1
P	19	6.2	0.6	20	7.1	0.1
Ti	8	1.9	0.06	[b]	2.4	0.2
V	19	4.5	0.08	[b]	5.3	0.1
Zn	6	11	0.09	7	10	0.2
Al	5	5.3	1	12	3	1
Cr	9	1.1	3	13	4.5	3
Fe	0.2	1.8	3	1.3	2.6	3
Mg	2.4	4.5	0.3	1.6	1.0	0.3
Mn	1.6	3.0	0.4	5.5	9	0.4
Ni	1.7	4.1	1	0.2	0.5	1
Li	−72	3	0.1	[b]	15	0.1
Pb	−77	3	1	[c]	[c]	0.7
Sr	−67	15	0.1	[b]	3	0.1
Zr	−73	1.5	0.7	[b]	13	0.3

[a] LOD: limit of detection.
[b] Accuracy was not assessed because reference concentrations were not available.
[c] Pb was not detected in SNi reference material.

one, until an additional work could improve this result. As expected, from the results discussed in Table 8, determination of Li, Pb, Sr and Zr in L-1 can be only qualitative because of the high (~70%) accuracy error obtained. In SNi sample, accuracy error was around or lower than 10% for most of elements (Co, Cu, Na, Zn, Al, Cr, Fe, Mg, Mn and Ni), except Ca (14%) and P (20%). As noted before, Li, Sr, Pb, Ti and V accuracy could not be evaluated because reference concentration is not given in SNi sample. Extra experiments are planned, in order to evaluate the accuracy of those elements by using another method, like for example the added-recovered method or by comparison with the concentrations determined by another implemented methodology with different chemical and physical principles.

Precision, calculated as the relative standard deviation of the average ($n=6$) concentration of the element, was very near or lower than 10% for mostly elements, except Sr (15%) in L-1; and K (15%) and Li (15%) in SNi sample.

At last, limit of detection was estimated as the concentration of the blank line intensity, measured from the matrix blank dissolution, plus three times the standard deviation. 5000 mg L^{-1} of Fe and 1900 mg L^{-1} of Mg in 4% (v/v) HNO_3 dissolutions were used as matrix blanks for L-1 and SNi samples, respectively. Limits of detection ranged from 0.06 mg kg^{-1} to 8 mg kg^{-1} in dependence of element and sample; which guaranteed a good detection of all elements, according to the expected concentrations.

4. Conclusions

Novel characteristics of the interfering effect due to Al+Cr+Fe+Ni and Mg+Fe+Ni complex matrices in dissolutions that simulated the major composition of laterite and serpentine mineral considered in this work, has been described. The predominant role of the principal component Fe on the matrix effect in laterite sample contrasted with the existence of an interaction effect between Mg and, probably, Fe in serpentine that modified the effect of the individual principal component Mg in the Mg+Fe+Ni complex matrix of this sample.

An ICP OES methodology for the simultaneous quantitative determination of Al, Ca, Co, Cu, Cr, Fe, K, Mg, Mn, Na, Ni, P and Zn in Cuban laterite and serpentine minerals has been developed. Additionally, V and Ti can be quantitatively determined in laterite; and Li, Sr and Zr can be detected in both mineral types; while Pb can be detected in laterite mineral.

Acknowledgements

This work has been performed in the frame of the International Cooperation Program of the Universidad Complutense de Madrid with the Universidad de la Habana; and also as part of the IMRE Project “Improvement of the reliability of the analysis of environmental samples and advanced materials”, 2011 IMRE convocation.

References

[1] http://www.ecured.cu/index.php/Níquel_en_Moa. (Consulted: September 16, 2013).
[2] O.S. Barzaga, A.M. Hernández, A. Merayo, Ciencias Holguín 14 (2010) 1–9.
[3] O. Coto, F. Galizia, I. Hernández, J. Marrero, E. Donati, Hydrometallurgy 94 (2008) 18–22.
[4] J.A.C. Broekaert, Spectrochim. Acta, Part B 55 (2000) 739–751.
[5] I.B. Brenner, S. Vats, A.T. Zander, J. Anal. At. Spectrom. 14 (1999) 1231–1237.
[6] ISCL—319:2010 Determination of Fe, Ni, Co, SiO_2, Al_2O_3, MnO, Cr_2O_3 and MgO in laterites and serpentines by ICP-AES. Fusion method. Quality Management System. UEB Laboratory, Geominera Oriente Enterprise, 2010.
[7] LRM-PT-01 Procedure for Determination of Fe, Ni, Co, SiO_2, MgO, Al_2O_3, Cr_2O_3 and MnO by ICP- OES in raw mineral for nickel industry, Central Laboratory of Minerals (LACEMI) “José Isaac del Corral”, 2006.
[8] A New Approach to the High Concentration Chloride Leaching of Nickel Laterites, Bryn Harris, Carl White, Mal Jansen, Duncan Pursell, Presented at ALTA Ni/Co 11 Perth, WA, 2006.
[9] A New Process for Cobalt—Nickel Separation, D.L Jones, T.M. McCoy, K.E Mayhew, C.Y. Cheng, K.R. Barnard, W. Zhang, ALTA, 2010.
[10] H. Hong, Z. Li, P. Xiao, Clays Clay Miner. 57 (2009) 602–615.
[11] P.J. Lamothe, T.L. Fries, J.J. Consul, Anal. Chem. 58 (1986) 1881–1886.
[12] M. Totland, I. Jarvis, K. Jarvis, Chem. Geol. 95 (1992) 35–62.
[13] F. Le Cornec, C. Riandey, M.L. Richard, Minéralisation par micro-ondes de matériaux géologiques (roches et sols) et comparaison avec les méthodes classiques de mise en solution, in: D. Rambaud (Ed.), L’échantillonnage du prélèvement à l’analyse, E-Publishing Orstom, Paris, 1994.
[14] J.L. Kathryn, J.H. Steve, Analyst 123 (1998) 103R–133R.
[15] M. Chen, L.Q. Ma, Soil Sci. Soc. Am. J 65 (2001) 491–499.

[16] H. Shun-feng, W. Xia, G. He-yan, J. Wei, Rock Miner. Anal. (2011) 465–468.
[17] W. Guo-xin, X. Yu-yu, W. Hui, L. Feng, W. Cheng, H. Qing, Rock Miner. (2011) 572–575.
[18] Z. Li-wei, X. Yu-rong, Z. Wei, L. Wei-ping, Yunnan, Geology (2010) 346–350.
[19] N. Ponce, I. Altarriba, D. Carrillo, Serie Geológica 1 (1988) 75–82.
[20] F. Roja, C. Santana, Rev. Tecnol. 18 (1988) 8–15.
[21] J.M. Mermet, Anal. Chim. Acta 250 (1991) 85–94.
[22] J.M. Mermet, J. Anal. At. Spectrom 20 (2005) 11–16.
[23] A. Väisänen, A. Ilander, Anal. Chim. Acta 570 (2006) 93–100.
[24] M. Grotti, C. Lagomarsino, J.M. Mermet, J. Anal. At. Spectrom 21 (2006) 963–969.
[25] I.B Brenner, A.T. Zander, Spectrochim. Acta, Part B 55 (2000) 1195–1240.
[26] M. Iglésias, T. Vaculovic, J. Studynkova, E. Poussel, J.M. Mermet, Spectrochim. Acta, Part B 59 (2004) 1841–1851.
[27] I.B. Brenner, A. Zander, M. Cole, A. Wiseman, J. Anal. At. Spectrom 12 (1997) 897–906.
[28] F.V. Silva., C.L. Trevizan, C.S. Silva., A.R.A. Nogueira., J.A. Nóbrega, Spectrochim. Acta, Part B 57 (2002) 1905–1913.
[29] J. Davies, R.D. Snook, J. Anal. At. Spectrom. 1 (1986) 325–330.
[30] J.L. Todolí, L. Gras, V. Hernandis, J. Mora, J. Anal. At. Spectrom. 17 (2002) 142–169.
[31] I.B. Brenner, M.Z.B. Maichin, G Knapp, J. Anal. At. Spectrom 13 (1998) 1257–1264.
[32] M.T. Larrea, B. Zaldívar, J.C. Fariñas, L.G. Firgaira, M. Pomares, J. Anal. At. Spectrom. 23 (2008) 145–151.
[33] M.E. Villanueva Tagle, M.T. Larrea Marín, O. Martin Gavilán, M.D. Durruthy Rodríguez, F. Calderón Piñar, M.S. Pomares Alfonso, Talanta 94 (2012) 50–57.
[34] L.C. Trevizan, J.A. Nóbrega, J. Braz. Chem. Soc 18 (2007) 678–690.